Electronic-structure multiconfiguration calculation of a small cluster embedded in a local-density approximation host

I. V. Abarenkov
Department of Theoretical Physics, St. Petersburg State University, Petrodvoretz, St. Petersburg 198904, Russia

V. L. Bulatov*
Atomistic Simulation Group, Department of Materials, Imperial College, London SW7 2BP, United Kingdom

R. Godby
Department of Physics, University of York, York YO1 5DD, United Kingdom

V. Heine, and M. C. Payne
Cavendish Laboratory, Madingley Road, Cambridge CB3 0HE, United Kingdom

P. V. Souchko
Department of Theoretical Physics, St. Petersburg State University, Petrodvoretz, St. Petersburg 198904, Russia

A. V. Titov
St. Petersburg Institute for Nuclear Physics, Gatchina, St. Petersburg 188350, Russia

I. I. Tupitsyn
Department of Theoretical Physics, St. Petersburg State University, Petrodvoretz, St. Petersburg 198904, Russia
(Received 14 November 1996)

The present paper proposes a method for electronic-structure calculations on a type of system that cannot be handled by present methods. It considers a system where a multideterminant wave function is essential for an atom or a small cluster of atoms embedded in a large system, normally a solid, which can be treated by density-functional methods such as with the local-density approximation (LDA). A suitable example is a transition-metal atom in a semiconductor or MgO host. In this method the embedding potential for the cluster is generated from a LDA calculation but applied in a multiconfiguration calculation. The method and the concept of the embedding potential are validated by application to a simple system of a cluster Li_2Mg_2 of four pseudoatoms. [S0163-1829(97)04828-5]

I. INTRODUCTION

Modern science and technology need an understanding of the structure and properties of atoms, clusters of atoms, and molecules in the bulk or on the surface of a solid. Obvious applications include impurity optical spectra, catalysis, corrosion, and crystal growth, but complex systems can also exhibit new properties such as size quantization and electronic Coulomb blockade, which are promising candidates for nanotechnology in microelectronics.

Quantum-mechanical *ab initio* calculations of the electronic structure and total energy of solids are proving evermore useful for understanding complex processes in solids, including those at surfaces. The calculations using the techniques for static and dynamic simulations based on those associated with Car and Parrinello[1] are remarkably successful, but involve essentially the local-density approximation[2,3] (LDA), for electron exchange and correlation, or a functional closely related to the LDA.

However, the situation becomes unsatisfactory when open-shell atoms or molecules are involved, e.g., an atom of a $3d$ transition element. The majority of the LDA-type methods rely on some simple population scheme of one-electron levels. At the same time, the most natural Aufbau principle quite often fails to provide the correct description of the ground state for systems with open-shell atoms, for example, in transition elements where there is competition between filling of the $3d$ and $4s$ shells. In that case a wave function mixing several or many determinants is essential for describing the many-electron energy levels (terms), e.g., for optical properties and some magnetic states, not the single determinant to which the LDA is usually referred. A suitable procedure for calculations including open-shell atoms is the multiconfiguration self-consistent field (MCSCF) method.[4,5] Unfortunately, the MCSCF method cannot be applied to a solid as it stands because the computing time scales very badly with the system size.

Nevertheless, if a solid contains only a few open-shell atoms, the MCSCF method could be applied not to the whole solid, but only to a small part of it. For these cases, a hybrid embedding scheme is proposed to incorporate the MCSCF method within solid-state calculations, the rest of which are performed using the LDA.

The idea of embedding has a long history. Almost every theory of point defects in crystals contains some embedding scheme, from the very simple to the rather sophisticated. We

will mention only a few of them that are most closely related to the present paper. Perhaps the first embedding was the Bethe crystal field.[6] Another paper that strongly influenced the embedding theory is the paper of Mott and Littleton.[7] Their continuum model is the basis of many embedding schemes (see, for example, Ref. 8 and references therein) to account for the long-range effects. Since then various embedding schemes have been designed within different approaches.

For the semiclassical treatment of the properties and processes in ionic solids the embedding scheme of Ref. 9 was developed, into which pair potentials derived from quantum-mechanical calculations[10] were incorporated later.

In the one-electron approximation the Green's-function method provides a very suitable tool for the problem of a defect in a crystal. This method was employed in the elegant approach of Inglesfield,[11,12] where the whole one-electron problem (Hartree-Fock or Kohn-Sham) was confined entirely to the defect region by transferring the boundary conditions from infinity to a surface surrounding the defect region. In the variational formulation of this approach the energy functional acquires an additional surface integral that directly leads to the embedding potential. The Green's-function method was also employed in the perturbed cluster method of Pisani *et al.*,[13] where the linear combination of atomic orbitals basis was used to convert the problem to matrix form. Then approximations were made in the matrix block representing the indented crystal and the total matrix problem was transformed to a problem for a comparatively small block representing the defect region embedded in the crystal. The essential feature of the perturbed cluster method is that the first-order reduced density matrix is evaluated directly from the Green's-function matrix.

In the many-electron approach the ''group function method''[14] is usually applied so that the wave function of the whole system is approximated by the antisymmetrized product of many-electron function of individual atoms (ions) constituting the system. To make the approximation tractable the ''strong orthogonality'' condition[14] is usually imposed. This approach was employed in developing the equations for the response, including exchange and polarization, of the rest of the crystal to the defect region,[15] resulting in the justification, improvement, and modification of the models for the long-range effects. The group function method, together with the *ab initio* model potential,[16] was employed to develop a scheme[17,18] for the ionic crystals calculations where every ion is considered as being immersed in the sum of the potentials due to the surrounding atoms. The potentials from the near ions include the Coulomb, exchange, and orthogonality contributions. The farthest ions are represented by the corresponding point charges. The variant of the model potential used implies that the nodal structure of functions is preserved and not smoothed out as in the conventional norm-conserving pseudopotential theory. This is a transparent approach, but is rather a method for the self-consistent calculation with correlations of the large cluster.

The embedding scheme of the present paper serves to interface two different many-electron methods, the LDA and the MCSCF method, and therefore it is based on the properties that are well defined in both theories, namely the electronic density and the potential. Let us specify in a little more detail the type of system to be discussed. We consider a host material that can be adequately treated by the LDA method, although some details of the present discussion will be written in terms of a more restricted type of crystal consisting only of closed-shell atoms, e.g., MgO. Suppose an atom with open shell is implanted in the bulk or on the surface of the solid. We shall assume that the influence of the impurity atom on the solid is a short-range one without long-range Coulomb tails. Moreover, we are interested only in those properties and processes that are confined to the impurity or its near vicinity and are influenced by the crystal environment. In the present paper, the properties of the system that depend on energy will be considered, namely, the total electronic energy of the system, its dependence on the geometry of the system, and a few lowest excitation energies.

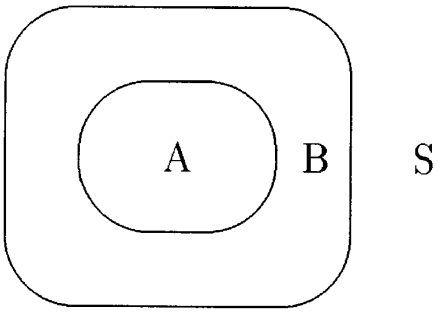

FIG. 1. Three regions: *A*, atoms; *B*, buffer; and *S*, solid.

II. OUTLINE OF THE METHOD

In our method different techniques (the MCSCF method and the LDA) are applied to different parts of the system (the impurity and host). Although *two* different techniques are applied, we propose to divide the whole system into *three* subsystems *A*,*B*,*S*, as follows. Subsystem *A* (atoms) (see Fig. 1) contains all the open-shell atoms and perhaps some atoms of the solid if their electronic structure is strongly influenced by the impurity. We assume that all the properties and processes to be considered are localized mostly in subsystem *A*. We assume also that the total charge associated with *A* does not differ from that in the ideal solid. Subsystem *S* (solid) contains all atoms of the solid where the influence of the impurity is negligible. The third subsystem, *B* (buffer), contains those atoms of the solid that are close to the impurity and experience its influence, but where this influence is comparatively small.

It should be noted that we define our subsystems in terms of the atoms assigned to them, not in terms of regions of space. We therefore do not introduce surfaces dividing one subsystem from another. Each subsystem is largely localized in its region of space (and we shall talk about regions *A*, *S*, and *B* in this loose sense), but its wave function can in principle extend over the whole space. Thus the wave function of, say, subsystem *A* is largely localized in region *A*, but it penetrates region *B* and so on. The degree of localization depends on the subsystem itself and on the influence of the other subsystems. For example, it is well known that the electronic density of an anion in an ionic crystal is more

compact than that of the free ion and the opposite is true for cations.

All atoms for which the LDA is unsatisfactory are collected in subsystem A and this has to be treated with the MCSCF method. Subsystem S can be adequately treated within the LDA approach as assumed for the pure solid. Subsystem B can be treated equally well with either the LDA or the MCSCF method.

The basic idea of the proposed approach is to apply to every subsystem the calculational method that suits it best and to simulate the influence of other subsystems with a potential that in this context is known as an embedding potential. The reason to introduce the third (buffer) subsystem B is to avoid matching the LDA and MCSCF wave functions and to allow the generation of the embedding potential to be carried out within one method of electronic-structure calculation. The potential V_S to embed A+B into S is generated with the LDA calculations of $B+S$ and the potential V_A to embed $B+S$ into A is generated with the MCSCF calculations of $A+B$.

Clearly, the influence of each subsystem on the other has to be calculated self-consistently. Therefore, the proposed combined MCSCF-LDA method can be expressed as the following sequence of steps.

(i) An appropriate estimate of the potential V_A simulating the influence of system A onto $B+S$ is made as an initial approximation. Quite often $V_A=0$ would be a suitable choice for an initial aproximation.

(ii) The $B+S$ system in the embedding potential V_A is calculated with the LDA method. The $B+S$ system is in fact an indented crystal with the indentation (big hole) where subsystem A was. Band-structure calculations with a supercell can be used in this case as is done for a crystal with a single impurity. Though the system actually calculated has periodically repeated indentations, still with a large enough supercell the influence of one indentation onto the others could be made negligible. The LDA provides the solution to the Kohn-Sham equations

$$\left(-\frac{\hbar^2}{2m_0}\nabla^2+V_{KS}^{(B+S)}+V_A\right)\psi_k=\epsilon_k\psi_k, \tag{1}$$

and the occupied Kohn-Sham orbitals ψ_k, $k=1,\ldots,N$, provide a full description of the $B+S$ system ground state in the LDA approximation. Equation (1), where $V_{KS}^{(B+S)}$ is the standard Kohn-Sham potential, has to be solved for the whole space. The occupied orbitals ψ_k are large over the space belonging to $B+S$ but penetrate the indentation (space belonging to A) in the same way as the Kohn-Sham orbitals for a crystal with a surface protrude into the vacuum. The degree and the way of this penetration depend on the particular shape of V_A.

(iii) The embedding potential V_S, simulating the influence of subsystem S onto B, is generated from the results of the calculations of step (ii). The Kohn-Sham orbitals obtained in step (ii) should first be reorganized into two sets, one belonging to B and one belonging to S. To do this orbitals $\phi_k^{(B)}$ and $\phi_k^{(S)}$ can be defined as linear combinations of ψ_k,

$$\phi_k^{(B)}=\sum_{m=1}^{N} C_{km}^{(B)}\psi_m, \quad k=1,\ldots,N_B$$

$$\phi_k^{(S)}=\sum_{m=1}^{N} C_{km}^{(S)}\psi_m, \quad k=1,\ldots,N_S \tag{2}$$

$$N_B+N_S=N,$$

with coefficients $C_{km}^{(B)}$ and $C_{km}^{(S)}$ comprising the square $N\times N$ matrix $\mathbf{C}$. The transformation (2) has to be made nonsingular in order that orbitals $\phi_k^{(B)}$ and $\phi_k^{(S)}$ together span the same functional space as the N orthogonal orbitals ψ_k. With the help of some localization procedure one can find coefficients $C_{km}^{(B)}$ and $C_{km}^{(S)}$ so that orbitals $\phi_k^{(B)}$ will have a much smaller value in region S compared to that in region B (i.e., they will be localized, with most of their weight in region B) and orbitals $\phi_k^{(S)}$ will have a much smaller value in B compared to that in S (localized in S). Our present assumption of a system of closed-shell atoms is involved in step (iii) because for a metal (for instance) one needs the whole band of occupied and unoccupied states to define localized orbitals such as Wannier functions. However, we believe our method can be extended to diamond-type semiconductors where the valence band can be expressed in terms of localized bonding orbitals.

There are a number of different localization procedures that can be used in setting up the $\phi_k^{(B)}, \phi_k^{(S)}$, one of which is the following. Consider, for example, the subsystem B. Using the orbitals $\phi_k^{(B)}$, $k=1,\ldots,N_B$, as trial Kohn-Sham orbitals for the isolated system B, one can adjust the coefficients $C_{km}^{(B)}$ so as to minimize the energy functional of the isolated system B calculated with the $\phi_k^{(B)}$. The obtained orbitals obviously would not satisfy the Kohn-Sham equations for the isolated system B exactly as their form is restricted to Eq. (2), but they will be localized in region B. Another possible localization procedure is to adjust the coefficients $C_{km}^{(B)}$ so that a one-determinant wave function built up from the $\phi_k^{(B)}$ would be as close as possible to the one-determinant wave function of the single system B. A similar localization procedure can be applied to system S also.

After the localized orbitals $\phi_k^{(B)}$ are obtained they are to be expressed as the solution of the equation

$$\left(-\frac{\hbar^2}{2m_0}\nabla^2+V_{KS}^{(B)}+V_A+V_S\right)\phi_k^{(B)}=\epsilon_k^{(B)}\phi_k^{(B)}. \tag{3}$$

Here $V_{KS}^{(B)}$ is the standard Kohn-Sham potential calculated with orbitals $\phi_k^{(B)}$, V_A was defined before, and the only unknown quantity is the embedding potential V_S. It can be obtained from Eq. (3) in several ways. One possibility is simply to invert Eq. (3) similarly to what is done in the well-known norm-conserving pseudopotential theory. Another possibility is to assume a suitable form for the potential V_S, say $\tilde{V}_S$, with parameters and to adjust the parameters so that the solutions $\tilde{\phi}_k^{(B)}$ of Eq. (3) with $\tilde{V}_S$ are as close as possible to the orbitals $\phi_k^{(B)}$ from Eq. (2).

One criterion of closeness is the minimum of the functional W,

$$W=\int |\rho^{(B)}(\mathbf{r})-\tilde{\rho}^{(B)}(\mathbf{r})|^2\tau(\mathbf{r})d\mathbf{r}, \tag{4}$$

where $\tau(\mathbf{r})$ is a weight function and

$$\rho^{(B)}(\mathbf{r})=\sum_{k=1}^{N_B}|\phi_k^{(B)}(\mathbf{r})|^2, \quad \tilde{\rho}^{(B)}(\mathbf{r})=\sum_{k=1}^{N_B}|\tilde{\phi}_k^{(B)}(\mathbf{r})|^2. \tag{5}$$

After the embedding potential V_S is constructed one can proceed with the next step.

(iv) The $A+B$ system in the embedding potential V_S is calculated with the MCSCF method.

Here the wave function Ψ of the system is calculated as a linear combination of many-electron functions of various configurations Ψ_k,

$$\Psi(x_1,\ldots,x_n)=\sum_k C_k\Psi_k(x_1,\ldots,x_n). \tag{6}$$

The list of configuration should be long enough to include all the configurations whose weights

$$w_k=|C_k|^2 \tag{7}$$

are essential.

The analog of the LDA electron density is the first-order spatial reduced density matrix

$$\begin{aligned}\rho(\mathbf{r}|\mathbf{r}')=n\int &\Psi(\mathbf{r}_1,\sigma_1,\mathbf{r}_2,\sigma_2,\ldots,\mathbf{r}_n,\sigma_n)\\ &\times\Psi^*(\mathbf{r}_1',\sigma_1,\mathbf{r}_2,\sigma_2,\ldots,\mathbf{r}_n,\sigma_n)d\sigma_1 d\mathbf{r}_2\\ &\times d\sigma_2\cdots d\mathbf{r}_n d\sigma_n.\end{aligned} \tag{8}$$

It can be transformed to the diagonal form

$$\rho(\mathbf{r}|\mathbf{r}')=\sum_n \lambda_n\psi_n(\mathbf{r})\psi_n^*(\mathbf{r}'). \tag{9}$$

Here $\psi_n(\mathbf{r})$ are the natural orbitals and λ_n are the natural occupation numbers. They provide all the information necessary to calculate the one-electron properties of the system.

It could be that the accuracy of the results obtained at this stage will already be good enough and calculations could be stopped here. If not, the calculations should be continued as follows.

(v) The embedding potential V_A, simulating the influence of subsystem A onto subsystem B is generated from the results of calculations of step (iv). For this the natural orbitals should be transformed into orbitals localized on subsystems A and B. After that the potential V_A should be constructed using a procedure similar to that for V_S in step (iii).

(vi) Return to step (ii) and proceed until convergence.

We have implemented this scheme with the LDA calculations performed using the CASTEP program[20] and the MC-SCF calculations performed using the MOLCAS program[21] and the numerical programs for atoms and diatomic molecules.[22]

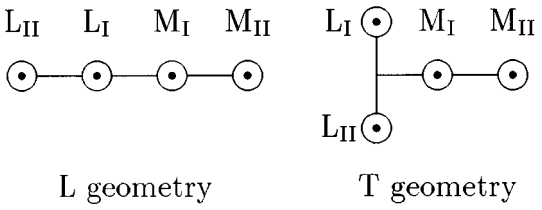

FIG. 2. Schematic geometries of the prototypical system.

III. PROTOTYPICAL SYSTEM

In order to test the method, we choose the simplest possible prototypical system, not only to reduce the scale of the computation, but also to analyze in detail what is going on. We also need it to be sufficiently small that we can do ''exact'' (within the necessary precision) calculations of the various excitation energies to compare the results of the present method with. In the whole calculation, the most resource-demanding part is that done with the MCSCF method and the computational cost is determined by the number of valence (''active'') electrons so that this number should be kept as low as possible. It is not necessary for the prototypical system to be a solid. Our proposed method could equally well be applied to a cluster or to a molecule, as long as the division into three subsystems is meaningful. Hence it is expedient to take for the prototypical system a cluster with the smallest possible number of atoms, every atom containing the smallest possible number of electrons, consistent with the other requirement that A should consist of open-shell atoms and that $B+S$ consist of closed-shell atoms or ions.

We therefore arrive at a minimal prototypical system as a cluster containing four atoms. Two identical lithiumlike atoms L_{I} and L_{II} with one electron each constitute subsystem A and we will be interested in the energy splitting between two singlet and one triplet states of this L_2 molecule. The closed-shell system $B+S$ consists of two magnesiumlike atoms M_{I} for B and M_{II} for S with two electrons each. We will consider two different geometries, linear L and transverse T, as shown in Fig. 2.

The core electrons were eliminated from consideration by representing the L^+ and M^{++} ions by ionic pseudopotentials in the conventional sense[19] and choosing the very simple form

$$V(r)=-Z\frac{1-\exp^{-\alpha r}}{r}, \tag{10}$$

with $Z_L=1$, $Z_M=2$ and $\alpha_L=0.619\,48$, $\alpha_M=0.693\,10$ to represent the first ionization potential of Li and the second ionization potential of Mg.

As it is not necessary to use the equilibrium geometry in the method developed, the internuclear separations were selected as a compromise between the calculated equilibrium

TABLE I. Coordinates of atoms in the prototypical system (in a.u.) in L and T geometries.

	L	T	
Atom	z	x	z
L_{II}	−6.548	−3.2745	0.000
L_{I}	0.000	3.2745	0.000
M_{I}	5.674	0.0000	5.674
M_{II}	10.478	0.0000	10.478

interatomic distances in the cluster and its parts, values of atomic radii, and the grid requirements in the CASTEP program. The coordinates of the atoms in both geometries are given in Table I, the z axis being directed along the line M_{I}-M_{II}.

The electronic structure of the prototypical system and its fragments (the M atom and L_2 and M_2 molecules) was investigated with the LDA, Hartree-Fock (HF), and MCSCF methods. The HF and MCSCF codes employed by us were designed for molecular calculations. The codes for an atom and for a diatomic molecule employ the numerical orbitals and could be applied immediately. The MOLCAS codes employ a Cartesian Gaussian basis set. The $10s6p1d$ and $10s7p2d$ basis sets were chosen for the L and M atoms, respectively, and these sets were optimized so as to bring the results of MOLCAS calculations for atoms and molecules as close as possible to that done with the numerical programs. MCSCF calculations were made with increasing numbers of configurations until convergence within 0.001 a.u. in the total energy was achieved, so we can consider the MCSCF results as exact. The number of configurations needed was of the order of 2×10^5 for the whole system and an order of magnitude less for its fragments. The MCSCF calculations for the whole system constituted the ''exact'' results with which the results from the present method could be compared.

The CASTEP code was designed for solid-state calculations and in order to apply it to an atom or a molecule this has to be enclosed in a large supercell. The cell was chosen as cubical with an edge length of 16 Å and atoms in both L and T geometries were arranged so that all the occupied orbitals practically vanish at the cell boundaries.

In what follows the many-electron states and one-electron states will be designated with the usual notations related to the corresponding symmetry group: central field symmetry for atom M, $D_{\infty h}$ for molecules L_2 and M_2, $C_{\infty v}$ for the prototypical system in L geometry, and C_{2v} for the prototypical system in T geometry.

TABLE II. Ground-state energies (in a.u.) of atom M and molecules M_2 and L_2.

	M	M_2	L_2
Method	^1S	$^1\Sigma_g^+$	$^1\Sigma_g^+$
HF	−0.752	−1.389	−0.365
LDA	−0.767	−1.433	−0.392
MCSCF	−0.783	−1.459	−0.401

TABLE III. Energies ΔE (in a.u.) of the lowest excitations of atom M and molecules M_2 and L_2 together with the difference $\Delta\epsilon$ of the lowest unoccupied and highest occupied Kohn-Sham levels.

	M		M_2		L_2
State	ΔE	State	ΔE	State	ΔE
^1P	0.135	$^1\Pi_g$	0.069	$^1\Sigma_u^+$	0.079
^3P	0.107	$^3\Pi_g$	0.057	$^3\Sigma_u^+$	0.017
$\Delta\epsilon$	0.112	$\Delta\epsilon$	0.059	$\Delta\epsilon$	0.036

The energies of the ground state of the M atom and the M_2 and L_2 molecules calculated in different approximations are given in Table II. From Table II it can be seen that the LDA method accounts for approximately 60–70 % of the correlations energy of the few-electron systems considered. The energy of the lowest singlet-singlet and singlet-triplet excitations, calculated as the difference of the total energies in the MCSCF method, are given in Table III. For comparison, the excitation energy calculated as the difference between the lowest empty and the highest occupied one-electron Kohn-Sham levels are also shown in this table. The results presented in Tables II and III confirm that the LDA method provides a reasonably accurate description of the systems it will be applied to in the present paper, namely, one M atom and the M_2 molecule. However, as expected, the LDA method is seen not to work so well for the L_2 molecule.

Several of the largest configuration weights are given for these fragments in Table IV, and in Table V the largest natural occupation numbers are shown. From Table IV one can see that there is one configuration (with a one-determinant wave function) that dominates for the M atom and for the M_2 molecule, whereas at least two configurations have comparable weights for the L_2 molecule. The natural occupation numbers from Table V also indicate that the wave functions of the M atom and M_2 molecule are close to the one-determinant function. However, the situation is very different with the L_2 molecule, where there are two electrons with

TABLE IV. Weights w_k of the most essential configurations for atom M and molecules M_2 and L_2 in the ground state.

k	M	M_2	L_2
1	0.953	0.898	0.841
2	0.037	0.023	0.139
3	0.009	0.011	0.014
4		0.009	0.006
5		0.007	
6		0.006	
7		0.005	
the rest	0.001	0.041	0.000
Total	1.000	1.000	1.000

TABLE V. Largest natural occupation numbers λ_n for atom M and molecules M_2 and L_2 in the ground state.

Orbital	M	Orbital	M_2	L_2
$1s$	1.907	$1\sigma_g$	1.907	1.681
$2p$	0.073	$1\sigma_u$	1.883	0.278
$2s$	0.018	$1\pi_u$	0.066	0.028
		$1\pi_g$	0.048	
		$2\sigma_g$	0.036	0.012
		$2\sigma_u$	0.027	
the rest	0.002	the rest	0.033	0.000
Total	2.000	Total	4.000	2.000

TABLE VI. Energies of the lowest states of prototype system (in a.u.).

L geometry		T geometry	
State	Energy	State	Energy
$^1\Sigma$	-1.833	$^1A_1$	-1.819
$^3\Sigma$	-1.811	$^3B_1$	-1.818
$^1\Sigma*$	-1.763	$^1B_1$	-1.791

opposite spins in the ground state and yet the occupation of the second orbital in the configurational mixing is considerable. This indicates that the one-determinant approximation for the L_2 molecule is a poor one even in its ground state.

The results of the full MCSCF calculations for the lowest few energy levels of the prototype system are given in Table VI. These constitute the exact answers with which to compare the results of the present method.

To show the necessity of the many-configuration wave function and the number of configurations involved let us consider the $^1A_1$ state in the T geometry as a typical example. In this state there are two configurations with weights 0.67 and 0.21, respectively. All other configurations have weight less than 0.01. However, in the one-configuration approximation (HF) the energy is -1.704 a.u. With the two mentioned configurations the energy is -1.740 a.u., which is still far from the converged value -1.819 a.u. These two configurations account for 30% of the correlation energy. In increasing the number of configurations, we found that as many as 2471 configurations were needed yield an energy of -1.798 a.u., i.e., to account for 80% of the correlation energy, and 35 465 configurations to yield an energy of -1.814 a.u. to account for 95% of the correlation energy. To take account of the last 5% of the correlation energy is was necessary to add another 100 000 configurations.

IV. APPLICATION OF THE PROPOSED METHOD TO THE PROTOTYPICAL SYSTEM AND DISCUSSION

In the prototypical system, subsystem A is the L_2 molecule and $B+S$ is the M_2 molecule, with the $M_{\rm I}$ and $M_{\rm II}$ atoms representing systems B and S, respectively. As step (i) the potential V_A was set equal to zero. The total energy, the electron density, the eigenfunctions, and the eigenvalues of the Kohn-Sham equation (1) were obtained for the M_2 molecule using the CASTEP code, as was explained in Sec. II as step (ii).

In the M_2 molecule there are two doubly occupied Kohn-Sham σ molecular orbitals $\psi_1(\mathbf{r})=\psi_{1\sigma g}(\mathbf{r})$ and $\psi_2(\mathbf{r})=\psi_{1\sigma u}(\mathbf{r})$. In step (iii) they were transformed into orbitals $\phi_1^{(B)}$ and $\phi_1^{(S)}$ localized on $M_{\rm I}$ and $M_{\rm II}$, respectively, using the second localization procedure described in Sec. II. The transformation (2) was chosen to be unitary and its parameters were adjusted to make $\phi_1^{(S)}(\mathbf{r})$ for atom $M_{\rm II}$ as close as possible to the Kohn-Sham orbital of the free atom M, which results in $\phi_1^{(S)}(\mathbf{r})$ being very nearly spherically symmetric. Then the orbital $\phi_1^{(B)}(\mathbf{r})$ is automatically defined. The functions defined in this way are not similar, even though the molecule M_2 is symmetric. The reason is that atoms $M_{\rm I}$ and $M_{\rm II}$ will be treated differently in the next stage of the calculation. Atom $M_{\rm II}$ will be removed and the embedding potential will be inserted instead to make the density of atom $M_{\rm I}$ in the embedding potential equal to $\rho^{(B)}(\mathbf{r})$.

The arguments why we choose to make atom $M_{\rm II}$ spherically symmetrical and not atom $M_{\rm I}$ are as follows. The electron density could not be divided exactly into two spherically symmetrical densities. By making $\rho_1^{(S)}(\mathbf{r})$ effectively spherically symmetric, the removal of subsystem S does not leave any long-range dipolar or quadrupolar, etc., tail. Therefore, if a potential exactly reproduces the density $\rho^{(B)}(\mathbf{r})$, this potential will be the embedding potential and there will be no need for corrections for any long-range tail of the $M_{\rm II}$ potential in the A region.

In the present case the embedding potential that must simulate the influence of the $M_{\rm II}$ atom onto the $M_{\rm I}$ atom resembles the pseudopotential for the virtual states of an atom, i.e., the pseudopotential for an extra electron added to the atom, and not for the electron of the atom. We have to think of this potential as, in general, nonlocal, or semilocal having different s, p, d, etc., components. In the case of atom M the occupied pseudostate is $1s$, by which we mean the lowest eigenvalue of the M pseudopotential corresponding to the real $3s$ Mg orbital. Its unoccupied (virtual) states are formally $2p$ and $2s$ and they have approximately the same energy. On the other hand, the $1s$ state of the embedding potential has to simulate the $2s$ virtual state, while the $2p$ state in the embedding potential must simulate the $2p$ virtual state. To achieve this, the s component of the embedding potential should be repulsive compared to the p component. In the case considered it was found that this semilocality can be reproduced by a local potential by using the fact that the s state and p state have different behavior near the origin because of the r^l factor. Hence a potential that is strongly localized in the vicinity of the origin has a significant effect on s states, but is almost negligible for p states. In the present paper the simplest form of the potential that has the required properties was chosen for the embedding potential. It is the sum of two exponentials centered at the position $\mathbf{R}$ of the $M_{\rm II}$ atom:

TABLE VII. Excitation energies (in a.u.) of the prototypical system L_2M_2, the isolated cluster L_2M, and the cluster in the embedding potential L_2M+V together with the ground-state energy change in the transition from L to T geometry.

Geometry	Transition	L_2M_2	L_2M	L_2M+V_{embed}
L	$^1\Sigma\rightarrow{}^1\Sigma^*$	0.070	0.074	0.070
T	$^1A_1\rightarrow{}^1B_1$	0.028	0.045	0.030
L	$^1\Sigma\rightarrow{}^3\Sigma$	0.022	0.019	0.023
T	$^1A_1\rightarrow{}^3B_1$	0.001	0.006	−0.001
	$L\ (^1\Sigma)\rightarrow T(^1A_1)$	0.014	0.010	0.014

TABLE VIII. Same as Table VII, except with the d orbitals removed from the basis.

Geometry	Transition	L_2M_2	L_2M	L_2M+V_{embed}
L	$^1\Sigma\rightarrow{}^1\Sigma^*$	0.071	0.075	0.070
T	$^1A_1\rightarrow{}^1B_1$	0.032	0.048	0.033
L	$^1\Sigma\rightarrow{}^3\Sigma$	0.022	0.019	0.023
T	$^1A_1\rightarrow{}^3B_1$	0.000	0.005	−0.001
	$L\ (^1\Sigma)\rightarrow T(^1A_1)$	0.016	0.010	0.015

$$\widetilde{V}_S=\widetilde{V}_S(\mathbf{r})=V_1e^{-\alpha_1|\mathbf{r}-\mathbf{R}|}+V_2e^{-\alpha_2|\mathbf{r}-\mathbf{R}|}, \tag{11}$$

with a comparatively small value of α_1 and negative V_1 and comparatively large value of α_2 and positive value of V_2. In this form, the first term accounts for the attraction common to both s and p states, and the second term is a repulsion that raises the s eigenvalue to that of the virtual s state as described above. The values of these parameters were chosen to reproduce approximately the density $\rho^{(B)}(\mathbf{r})$. To do this, for a given set of potential parameters $\alpha_1,\alpha_2,V_1,V_2$, the Kohn-Sham equation was solved for the M_{I} atom in the field of the potential $\widetilde{V}_S$ of Eq. (11), the orbital $\widetilde{\phi}_1^{(B)}(\mathbf{r})$ was obtained, and the density $\widetilde{\rho}^{(B)}(\mathbf{r})=|\widetilde{\phi}^{(B)}{}_1(\mathbf{r})|^2$ was calculated. The functional (4) with the simplest form

$$\tau(\mathbf{r})=e^{-\beta|\mathbf{r}-\mathbf{R}_1|}+e^{-\beta|\mathbf{r}-\mathbf{R}_2|} \tag{12}$$

for the weight function was minimized with respect to the potential parameters. Here $\mathbf{R}_1$ and $\mathbf{R}_2$ coincide with the position vectors of the L_{I} and L_{II} atoms in the T geometry and $\beta=1.0$ a.u. The optimum values of the potential parameters were found to be $V_1=-0.26$ a.u., $\alpha_1=0.43$ a.u., $V_2=18.4$ a.u., and $\alpha_2=1.256$ a.u. This potential is well localized. It is centered on the M_{II} atom and has a radius of 2.5 a.u. At the same time the distance between the M_{II} and M_{I} atoms is 5 a.u. and the distance between the M_{II} atom and the L_2 molecule is 10 a.u. The obtained potential reproduces the density $\rho^{(B)}(\mathbf{r})$ moderately well. To fit the density $\rho^{(B)}(\mathbf{r})$ more accurately, a better potential that is both nonlocal and contains more flexible radial components should be used. Still, even our simple potential (11) does very well, as we will see , and can serve as an embedding potential for the chosen prototypical system. Thus step (iv) is completed.

Two sets of calculations were performed in the present investigation. In the first set the M_{II} atom was removed completely from the system and the ground and few first excited states of molecule L_2M were calculated in both geometries as isolated three-atom clusters. In Table VII the excitation energies for the singlet-singlet and singlet-triplet excitations together with the difference of the ground-state energies in L and T geometries are given for the prototypical system (L_2M_2) and for the system in the isolated cluster approximation (L_2M). One can see from the table that all the energy differences have changed when the isolated cluster approximation is applied. Some changes are noticeable but small: others, for example, the $^1A_1\rightarrow{}^1B_1$ transition energy in the T geometry, are comparatively large, constituting up to 50% of the transition energy itself. This clearly shows the necessity for the embedding potential.

The second set of calculations employs the present combined MCSCF-LDA scheme. The simple local embedding potential constructed in step (iv) was used to simulate the M_{II} atom that has been removed. This is step (v) of the proposed method. The ground state and the same excited states were calculated for both geometries. The calculated excitations energies and difference of the ground-state energies in L and T geometries for this case are also given in Table VII. In both sets of calculations the same basis set was employed, which coincides with the set used in the L_2M_2 calculations.

In order to test the influence of the finite basis set the calculations were repeated with a smaller basis set obtained by removing the d basis functions. The results for the excitation energies in this case are given in Table VIII. This table shows that the excitations energies are almost unchanged with the basis set reduction, although changes in the absolute values of the energy constitute several units in the last decimal place shown in the table.

Inspection of the tables shows that the embedding potential added to the isolated cluster moves all the excitation energies and the difference of the ground-state energies in the L and T geometries close to their exact values in the total system. The difference between the values obtained in the proposed method and the exact ones are of the order 0.05 eV.

It should be stressed that the same embedding potential was applied in the calculation of all the different states and in the different geometries. It is also worth mentioning that the embedding potential has a very simple form. It reproduces the energies of different states of the system quite well, even of those states that are not completely localized in the A region, e.g., the excited $^1\Sigma^*$ state in the L geometry. The reproduction of the spatial distribution of the electron density is less satisfactory. The latter can be improved by using a more complicated, nonlocal form of the embedding potential.

V. CONCLUSION

In this paper two geometries L and T geometry were employed in order to show that the results do not depend on the

quasi-one-dimensional character of the prototypical system in the L geometry. We may therefore conclude that the combined MCSCF-LDA method proposed in the present paper is valid and can be applied to an open-shell impurity in the closed-shell host crystal. The application of the method to the noble- and transition-metal impurities in insulators will be the subject of subsequent papers.

ACKNOWLEDGMENTS

This work was made possible by the Royal Society (London) through a joint project grant, which is gratefully acknowledged. The work was also supported in part by a NATO grant, by NATO Collaborative Research Grant No. 960521, and by the Russian Fund for Fundamental Investigations Grant No. 96-03-34074.

*Permanent address: Department of Theoretical Physics, St. Petersburg State University, Petrodvoretz, St. Petersburg 198904, Russia. Present Address: Physics Department, Oregon State University, Corvallis, OR 97331-6507.

[1] R. Carr and M. Parrinello, Phys. Rev. Lett. **55**, 2471 (1985).

[2] R. M. Dreizler and E. K. U. Gross, *Density Functional Theory* (Springer-Verlag, Berlin, 1990).

[3] R. G. Parr and W. Yang, *Density-Functional Theory of Atoms and Molecules* (Oxford University Press, New York, 1989).

[4] R. Sheppard, in *Ab Initio Methods in Quantum Chemistry*, edited by K. P. Lawley (Wiley, London, 1987), Vol. II, p. 63.

[5] B. O. Roos, in *Ab Initio Methods in Quantum Chemistry* (Ref. 4), p. 399.

[6] H. Bethe, Ann. Phys. (Leipzig) **3**, 133 (1929).

[7] N. F. Mott and M. J. Littleton, Trans. Faraday Soc. **34**, 485 (1938).

[8] L. N. Kantorovich and A. L. Shluger, Phys. Rev. B **53**, 136 (1996).

[9] *Computer Simulation of Solids*, edited by C. R. A. Catlow and W. C. Mackrodt, Lecture Notes in Physics Vol. 166 (Springer, Berlin, 1982).

[10] J. D. Gale, C. R. A. Catlow, and W. C. Mackrodt, Model. Simul. Mater. Sci. Eng. **1**, 45 (1992).

[11] J. E. Inglesfield, J. Phys. C **14**, 3795 (1981).

[12] G. A. Baraff and M. Schlüter, J. Phys. C **19**, 4383 (1986).

[13] C. Pisani, R. Dovesi, R. Nada, and L. N. Kantorovich, J. Chem. Phys. **92**, 7448 (1990).

[14] R. McWeeny, *Methods of Molecular Quantum Mechanics* (Academic, New York, 1992).

[15] L. N. Kantorovich, J. Phys. C **21**, 5041 (1988); **21**, 5057 (1988).

[16] S. Husinaga, L. Seijo, Z. Barandiarán, and M. Klobukowski, J. Chem. Phys. **86**, 2132 (1987).

[17] Z. Barandiarán and L. Seijo, J. Chem. Phys. **89**, 5739 (1988).

[18] S. López-Moraza, J. L. Pascual, and Z. Barandiarán, J. Chem. Phys. **103**, 2117 (1995).

[19] V. Heine, Solid State Phys. **24**, 1 (1970).

[20] M. C. Payne, M. P. Teter, D. C. Alan, T. A. Arias, and J. D. Joannopoulos, Rev. Mod. Phys. **64**, 1045 (1992).

[21] K. Anderson, M. R. A. Blomberg, M. P. Fülsher, V. Kellö, R. Lindh, P.-Å. Malmqvist, J. Noga, J. Olsen, B. O. Roos, A. J. Sadlei, P. E. M. Siegban, M. Urban, and P.-O. Windmark, MOLCAS, Version 2, University of Lund, 1991.

[22] S. Kotochigova and T. Tupitsyn, Int. J. Quantum Chem. **29**, 307 (1995).